Purification, Characterization, and Synthesis of an Inward-Rectifier K^+ Channel Inhibitor from Scorpion Venom†

Zhe Lu and Roderick MacKinnon*

Department of Neurobiology, Harvard Medical School, 220 Longwood Avenue, Boston, Massachusetts 02115

Received February 6, 1997; Revised Manuscript Received April 16, 1997⊗

ABSTRACT: We have purified a protein inhibitor of an inward-rectifier K^+ channel, ROMK1, from the venom of the scorpion *Leiurus quinquestriatus* var. *hebraeus.* The inhibitor is Lq2, a previously discovered blocker of voltage- and Ca^{2+}-activated K^+ channels. Mutations were made on the channel and the inhibitor, and the resulting effects were examined using an electrophysiological assay. The data show that Lq2 blocks the pore of ROMK1, and that the interaction surface on Lq2 is the same for binding to inward-rectifier, voltage-activated, or Ca^{2+}-activated K^+ channels. These findings support the notion that different classes of K^+ channels have different gates but a similar K^+-selective pore structure.

A large number of naturally-occurring inhibitors have been isolated to study ion channels. The venoms of a variety of poisonous animals have been a particularly rich supply of fascinating proteins that bind to and interfere with normal ion channel function. These inhibitors tend to be small (less than 100 amino acids), are compactly folded, and contain multiple disulfide bridges. They are very specifically directed against either K^+, Na^+, Ca^{2+}, or other channel types (*1*).

Potassium channels fall into two main structural classes based on hydropathy analysis of their main pore-forming subunits (*2*). The voltage- and Ca^{2+}-activated K^+ channels form one class having six membrane-spanning segments in each of four subunits (3, 4). The inward-rectifier K^+ channels (including G-protein-activated K^+ channels) make up the second class, having only two membrane-spanning segments per subunit in the tetramer (*5*). Numerous inhibitors of voltage- and Ca^{2+}-activated K^+ channels have been discovered, especially from the venoms of scorpions (charybdotoxin and its isoforms) and snakes (dendrotoxins) (*1*). On the other hand, no protein inhibitors of inward-rectifier K^+ channels have been described. We therefore set out to identify and purify an inward-rectifier K^+ channel inhibitor for the purpose of studying the function and structure of the channel.

MATERIALS AND METHODS

Channel Expression in Xenopus Oocytes. Oocytes dissected from *Xenopus laevis* frogs were incubated in a collagenase (2 mg/mL; Worthington)-containing saline solution (NaCl, 82.5 mM; KCl, 2.5 mM; $MgCl_2$, 1.0 mM; HEPES, 5.0 mM; pH 7.6). Oocytes were agitated on a platform shaker (120 rpm) for about 90 min and then rinsed thoroughly with and stored in a gentamicin (50 μg/mL; Gibco-BRL)-containing solution (NaCl, 96 mM; KCl, 2 mM; $CaCl_2$, 1.8 mM; $MgCl_2$, 1 mM; HEPES, 5 mM; pH 7.6). Defolliculated oocytes were selected at least 2 h after the collagenase digestion. RNA injection of oocytes was carried out at least 16 h later. The injected oocytes were stored at 18 °C.

Electrophysiological Recording. The ROMK1 and the IRK1 channels were studied using a two-electrode voltage clamp (Oocyte Clamp OC-725B, Warner Instrument Corp.). The resistance of electrodes, filled with 3 M KCl, was 0.3−0.6 MΩ. Channel currents were elicited by hyperpolarizing the membrane from the holding potential (about 0 mV) to −80 mV (50−150 ms) and then depolarizing to 80 mV (50 ms). The electrical signal was filtered at 1 kHz using an 8-pole Bessel filter (Frequency Devices Inc.) and sampled at 5 kHz using an analog-to-digital converter (Indec Systems, Inc.) interfaced with a personal computer. Background leak currents were obtained by exposing oocytes to a high concentration of Lq2 (see Results). The bath solution contained KCl,100 mM; $CaCl_2$, 0.3 mM; $MgCl_2$, 1.0 mM; and HEPES, 10 mM; pH 7.6. Lq2 concentration was calculated using the extinction coefficient 8.6 mM^{-1} cm^{-1} at 280 nm wavelength (see below). All toxin-containing solutions were freshly diluted from stock solutions.

Mutagenesis and RNA Preparation. The ROMK1 and IRK1 cDNAs were cloned into the p-SPORT1 (Gibco-BRL) and the pcDNA1/AMP (Invitrogen) plasmids, respectively (*6*, *7*). A mutation was introduced into the ROMK1 cDNA to create an *Nde*I site without altering the amino acid sequence. Mutations were produced in the channel gene using the polymerase chain reaction (PCR) primed with a mutagenic oligonucleotide. A 240 base pair fragment containing the mutation (between *Nde*I and *Bgl*II) was subcloned into a wild-type recipient version of the channel gene and was sequenced. RNA for ROMK1 and IRK1 was synthesized from *Not*I-linearized cDNA using T7 RNA polymerase (Promega).

Purification of the Inhibitor. The peptide purification was carried out following a protocol described previously (*8*). Lyophilized venom of the scorpion *Leiurus quinquestriatus* var. *hebraeus* was dissolved in 20 mM sodium borate (pH 9.0) at a concentration of 20−100 mg/mL. The sample was vortexed and then centrifuged at 27000*g* for 10 min. The supernatant was filtered through a Millex filter with a pore

† This work was supported by an NIH grant (GM43949).

* Address correspondence to this author at Rockefeller University, Box 47, 1230 York Ave., New York, NY 10021. Telephone: 212-327-7287. FAX: 212-327-7289. Email: mackinn@rockvax.rockefeller.edu.

⊗ Abstract published in *Advance ACS Abstracts,* May 15, 1997.

S0006-2960(97)00284-5 CCC: $14.00

size of 0.2 μm (Millipore) and then fractionated using a Mono-S FPLC column (HR 5/5, Pharmacia LKB Biotechnology Inc.). The active fraction was further separated using a reverse-phase HPLC column (C8, 0.46 × 25 cm, 5 μm, 300 Å pore size, Beckman). All fractions were collected, lyophilized, and then resuspended in 50 mM sodium phosphate (pH 7.0) for the subsequent assay. The yield of Lq2 was 37 μg per 100 mg of lyophilized venom. About 400 mg of the venom was used in the study. The purity of the active fraction was examined using a reverse-phase HPLC. The mass of the purified material determined on a VG analytical MALDI-TOF spectrometer is 4347 Da (predicted mass of Lq2 is 4345).

Preparation of the Recombinant Lq2. A gene for Lq2 (CCATTCACCCAGGAATCGTGCACCGCTAGCAACCAGTGCTGGTCC ATATGCAAGCGCCTGCACAACACCAACCGCGGTAAATGCATGAACAAAAAATGCCGTTGCTACTCC) was made from two synthetic oligonucleotide duplexes and inserted into the pCPS105 vector (*Sal*I−*Hind*III)(*9*). To generate a mutation, a PCR-generated and sequenced Lq2 gene containing the desired mutation was used to replace the wild type gene (*Sal*I−*Hind*III). Lq2 was prepared and purified according to a previously described method with some minor modifications (9,10). Lq2 protein was produced as a fusion protein in *Escherichia coli* strain BL21. The fusion protein was purified using DEAE-cellulose column chromatography. After a 16−24 h dialysis against a buffer solution (Tris, 10 mM; β-mercaptoethanol, 0.5 mM; pH 7.0), NaCl (100 mM), $CaCl_2$ (1 mM), and trypsin (5 μg/mg of fusion protein; Worthington) were added and incubated at room temperature (22 ± 1 °C) for 1 h. [The fusion carrier protein and Lq2 are connected by a factor Xa cleavage site (Ile-Glu-Gly-Arg) that can also be efficiently cut by trypsin.] Lq2 was purified partially from the trypsin-digested mixture using an SP-Sephadex (C25) column (a pH step gradient from 9.0 to 12.0). To facilitate N-terminal glutamine cyclization, Lq2 was incubated in 5% acetic acid at 65 °C for 4 h. Lq2 was subsequently purified using reverse phase HPLC (Beckman C18, 0.46 × 25 cm, 5 μm, 80 Å pore size). The mass of recombinant Lq2 determined on a VG analytical MALDI-TOF spectrometer is 4345 Da, identical to the predicted one.

Recombinant noxiustoxin, agitoxin 1, and agitoxin 2 were made in a similar way, but without the N-terminal cyclization step. Recombinant charybdotoxin, iberiotoxin, and margatoxin were provided by M. Garcia.

Amino Acid Analysis and Determination of the Extinction Coefficient. The amino acid analysis was done using a 420A derivatizer and a 130A separation system (Applied Biosystems) (Table 1). The extinction coefficient for recombinant Lq2 was calculated by determining the amino acid composition of an aliquot of toxin of known absorbance. The values are 8.6×10^{-3} M^{-1} cm^{-1}, 1.8×10^{-2} M^{-1} cm^{-1}, and 3.9×10^{-2} M^{-1} cm^{-1} at 280 nm, 235 nm, and 215 nm, respectively.

RESULTS

A Peptide Inhibitor (Lq2) Inhibits the ROMK1 Channel. We screened the venom from a variety of scorpions for its ability to inhibit the ROMK1 channel. The venom from the scorpion *Leiurus quinquestriatus* var. *hebraeus* contained inhibitory activity. We purified the active component using two sequential chromatographic steps, cation exchange FPLC

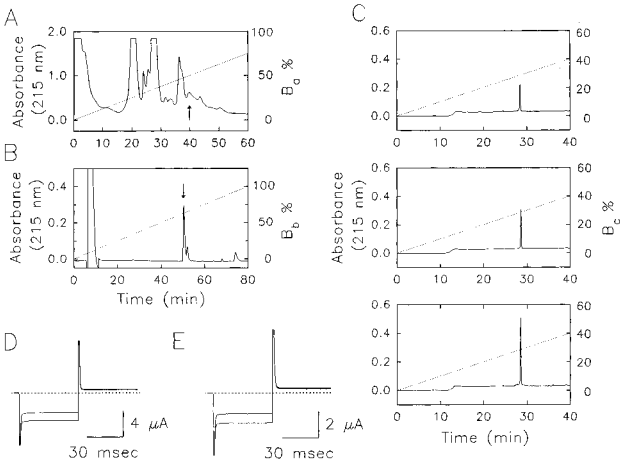

FIGURE 1: Purification and identification of the inhibitor. (A) A Mono-S chromatograph of the venom suspension described under Materials and Methods. Buffer A_a contained 20 mM sodium borate, pH 9.0; buffer B_a contained 0.5 M NaCl and 20 mM sodium borate, pH 9.0. The flow rate was 2 mL/min. The dashed line corresponds to the solvent gradient. The active fraction is indicated by the arrow. (B) C8 reverse phase chromatograph of the active fraction from panel A. Buffer A_b contained 0.1% trifluoroacetic acid (TFA); buffer B_b contained 10% acetonitrile, 5% isopropyl alcohol, and 0.1% TFA. (C) A series of C18 reverse phase chromatographs. The samples were the active material purified in panel B (upper), recombinant Lq2 (middle), and the combination of both (lower). Buffers A_c and B_c were 0.1% TFA in water and acetonitrile, respectively. The flow rate was 0.5 mL/min for both panels B and C. (D and E) Currents were elicited from oocytes injected with ROMK1-N171D RNA by stepping the membrane voltage from 0 mV (the holding potential) to −80 mV (50 ms) and then to 80 mV (50 ms). The lower and upper traces were recorded in the absence and presence of the purified material from panel B (0.15 μM, panel D) and recombinant Lq2 (0.15 μM, panel E). The two experiments were done in two separate oocytes. Dashed lines identify the zero current level.

(MONO-S) followed by reverse phase HPLC (C-8) (Figure 1A,B). Figure 1D shows the effect of the purified inhibitor on currents through a mutant channel (ROMK1-N171D) expressed in an oocyte.

The wild-type ROMK1 channel is a weakly rectifying channel that conducts current at all experimently achievable voltages in oocytes. Since some endogenous oocyte channels producing the background leak currents are also open at all voltages, it was difficult to separate ROMK1 currents from the background. To overcome this problem, in our initial screen we used the ROMK1-N171D channel that is highly conductive at negative but not positive voltages (*11*, *12*). Thus, the quantity of outward current at positive voltages was used to approximate the leak current at the negative voltages.

Mass spectrometry (MW = 4347; Materials and Methods), amino acid analysis (Table 1), chromatographic behavior (Figure 1C), and specific activity (Figure 1D,E) showed that the "new" inhibitor of the ROMK1 inward-rectifier K^+ channel is identical to Lq2, a previously discovered toxin. Lq2 was originally identified as an inhibitor of Ca^{2+}-activated K^+ channels and subsequently was shown also to block voltage-activated K^+ channels (*10*, *13*).

Specificity of the Interaction between Lq2 and the Channel. Figure 2A shows blockade of the ROMK1-N171D channel by Lq2 (3.5 μM). In contrast, a closely related inward-rectifier K^+ channel, IRK1, was relatively insensitive to Lq2 (Figure 2A). Furthermore, six different (but structurally

Table 1: Amino Acid Analysis[a]

	residues/molecules		
	observed		
	native material	Lq2	theoretical
Asp, Asn	3.7	3.9	4
Glu, Gln, pGlu	3.8	4.3	4
Ser	3.7	3.8	4
Gly	1.2	1.1	1
His	1.0	1.1	1
Arg	3.1	3.2	3
Thr	3.1	2.9	3
Ala	1.1	1.1	1
Pro	0.1	0.1	0
Tyr	0.9	0.9	1
Val	0.0	0.0	0
Met	1.1	1.0	1
Iso	0.8	0.7	1
Leu	1.0	1.0	1
Phe	1.1	1.1	1
Lys	4.3	4.3	4

[a] The contents of cystine and tryptophan were not determined. pGlu stands for pyroglutamate.

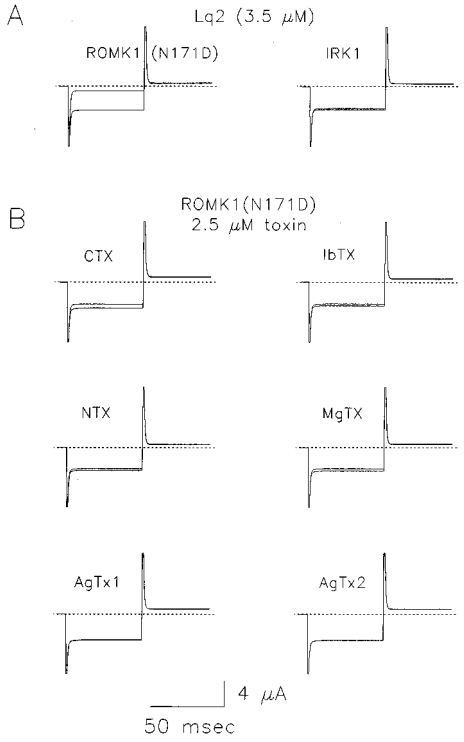

FIGURE 2: Specificity of the ROMK1−Lq2 interaction. The voltage protocol was the same as in Figure 1. (A) Current traces of the ROMK1-N171D channel (left) and the IRK1 channel (right) were recorded in the absence and presence of 3.5 μM Lq2. Recordings were made in two separate oocytes. (B) Current traces of the ROMK1-N171D channel were recorded in the absence and presence of 2.5 μM toxins as indicated. (CTX, IbTx, NTX, MgTx, AgTx1, and AgTx2 refer to charybdotoxin, iberiotoxin, noxiustoxin, margatoxin, agitoxin 1, and agitoxin 2, respectively.) All current traces of the ROMK1-N171D channel in panels A and B were recorded from the same oocyte.

similar) scorpion toxins (charybdotoxin, CTX; iberiotoxin, IbTx; noxiustoxin, NTX; margatoxin, MgTx; agitoxin 1, AgTx1; and agitoxin 2, AgTx2; at 2.5 μM) had little effect on the ROMK1-N171D channel (Figure 2B). These results show that the interaction between Lq2 and the ROMK1 channel is specific.

Figure 3 shows the concentration dependence of wild-type ROMK1 inhibition by Lq2. The dependence is consistent

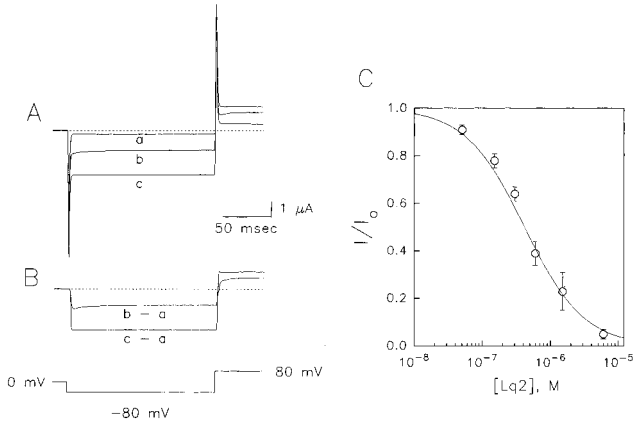

FIGURE 3: Determination of the affinity of the wild-type ROMK1 channel for Lq2. (A) ROMK1 currents were elicited using the voltage protocol shown below. Current traces were recorded in the absence and presence of Lq2 (>50 μM, a; 0.5 μM, b). Higher concentrations of Lq2 did not further reduce the current beyond that shown in trace a. The current traces of b and c, after subtracting trace a, are shown in panel B. (C) The fraction of unblocked current, I/I_o, (mean ± SEM; $n = 3-7$), is plotted as a function of Lq2 concentration. All data were corrected for background leak current using the high Lq2 concentration protocol described above. The curve superimposed on the data corresponds to the best fit (least-squares) using the equation $I/I_o = K_i/(K_i + [Lq2])$, where [Lq2] is Lq2 concentration. The inhibition constant (K_i) is 0.41 μM.

with a 1:1 binding stoichiometry between the channel and toxin, as was shown for the voltage- and Ca^{2+}-activated K^+ channels. In this case, the equilibrium dissociation constant is 0.4 μM. Figure 3A,3B shows how the background oocyte current was subtracted from the total current to ensure an accurate measurement of the ROMK1 current.

Mutations in the ROMK1 P-Region Affect the Channel Affinity for Lq2. We tested whether Lq2 blocks the ROMK1 channel through binding to its P-region. Because the Shaker K^+ channel is very sensitive to Lq2 (*10*) and the IRK1 channel is insensitive (Figure2), we designed ROMK1 mutations mainly by comparing their P-region sequences with that of the ROMK1 channel. The K^+ channel signature sequence (T-X-X-T-X-G-Y/F-G) (*14*) was used as a reference to align the sequences, and one or two residues at a time were mutated. Figure 4 shows two examples of mutant ROMK1 channels. Channels containing the mutations E151D/Q152E had wild-type-like affinity for Lq2 while the mutant E123S/N124E was relatively insensitive. A summary of all channel mutations is given in Figure 5A. Changes in the free energy of toxin binding (RT units) resulting from the channel mutations are shown in Figure 5B. We do not know the mechanisms by which the mutations affect the toxin affinity. One of the mutations (N117A) alters an N-linked glycosylation consensus sequence (*6*, *15*). Nevertheless, these results argue that Lq2 inhibits the ROMK1 channel by binding to the structure formed by the P-region.

Effects of Mutations on the Toxin. Studies on several Lq2 isoforms, including charybdotoxin (*16*−*18*), agitoxin 2 (*19*, *20*), and kaliotoxin (*21*), have identified amino acids that contact voltage- and Ca^{2+}-activated K^+ channels. These interaction residues are located on a wedge-shaped surface on the toxin structure—the wedge is thought to protrude into a shallow concavity that would comprise the extracellular pore entryway (*20*). To address whether Lq2 interfaces the ROMK1 channel with a similar orientation, four amino acids on the toxin were mutated individually to alanine. Three of

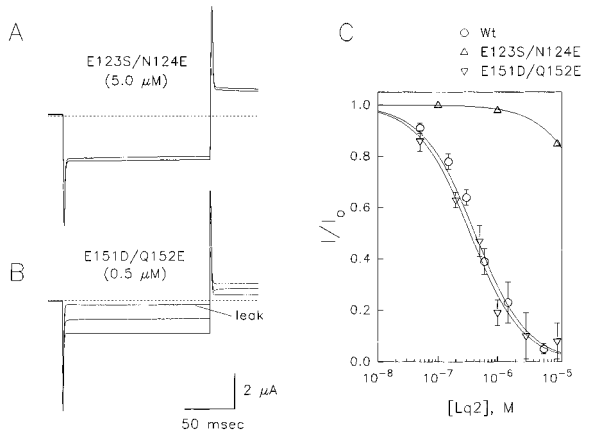

FIGURE 4: ROMK1 P-region mutations affect Lq2 affinity. (A and B) The current traces of two double-mutant channels (E123S/N124E, panel A; E151D/Q152E, panel B) were recorded in the absence and presence of Lq2 at the concentrations indicated. The voltage protocol was the same as in Figure 3. The leak current trace was obtained using high concentrations of Lq2 (see Figure3). (C) The fraction of unblocked current (mean ± SEM; $n = 3-7$) for the wild-type and two mutant channels is plotted as a function of Lq2 concentration. The curves superimposed on the data correspond to the best fits (least-squares) using the equation $I/I_o = K_i/(K_i + [Lq2])$. The estimated K_i values are 0.41 μM, 0.35 μM, and *about* 50 μM for the wild-type channel, E151D/Q152E channel, and E123S/N124E channel, respectively. Background leak current correction was not applied to the E123S/N124E mutant channel so the K_i value for this channel is less accurate.

A

Channels	Lq2 K_i (μM)	Channels	Lq2 K_i (μM)
Wild type	0.40 ± 0.05 (n=14)	S130A*	1.08 ± 0.08 (n=15)
N117A*	1.77 ± 0.14 (n=6)	S130D	0.25 ± 0.02 (n=8)
R118A*	0.59 ± 0.05 (n=12)	I142L*	0.95 ± 0.19 (n=4)
E123S/N124E	≈ 50 (n=3)	Y144F*	0.71 ± 0.03 (n=5)
E123A*	≈ 50 (n=4)	F146A*	≈ 30 (n=7)
N124A*	≈ 15 (n=4)	F146D	≈ 30 (n=4)
N124G	≈ 15 (n=4)	F148C*	5.14 ± 0.48 (n=5)
N126E*	0.25 ± 0.04 (n=9)	E151D/Q152E*	0.36 ± 0.06 (n=10)
G127S*	0.40 ± 0.04 (n=12)		

B

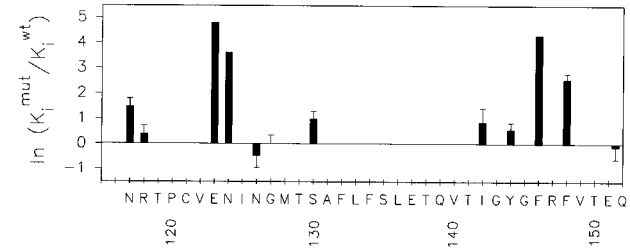

FIGURE 5: Summary of ROMK1 P-region mutations. (A) All K_i values (mean ± SEM; $n = 3-20$) were calculated using the equation $K_i = [Lq2]\Theta/(1 - \Theta)$, where $\Theta = I/I_o$. In most cases, Lq2 at concentrations near K_i were used, and K_i values were calculated using the leak-subtracted data. For the low-affinity mutant channels, Lq2 at 5−10 μM was used, and background leak current correction was not applied. The K_i values were thus rough estimations (labeled with "≈"). The data indicated with asterisks were used to construct plot B in which the free energy changes (in RT units) due to the mutations are plotted against the primary sequence.

these residues (Arg 25, Lys 27, and Asn 30) correspond to functionally important binding residues on CTX (*17*), a toxin which differs from Lq2 by only eight amino acids. The fourth mutated residue (Arg 19) corresponds to a residue on the "back side" of CTX. The outcome of these mutations is shown in Figure 6, and is in reasonable agreement with

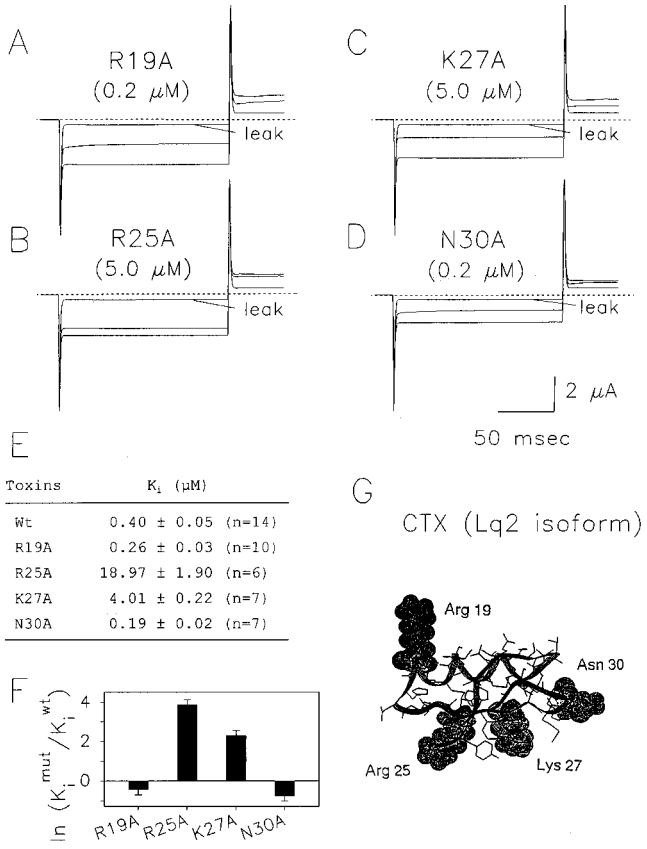

E

Toxins	K_i (μM)
Wt	0.40 ± 0.05 (n=14)
R19A	0.26 ± 0.03 (n=10)
R25A	18.97 ± 1.90 (n=6)
K27A	4.01 ± 0.22 (n=7)
N30A	0.19 ± 0.02 (n=7)

H

```
CTX  ZFTNVSCTTSKECWSVCQRLHNTSRGKCMNKKCRCYS
LQ2  ZFTQESCTASNQCWSICKRLHNTNRGKCMNKKCRCYS
```

FIGURE 6: Effects of Lq2 mutations on the ROMK1−Lq2 interaction. (A−D) The current traces for the ROMK1 channel were recorded in the absence and presence of four different mutants of Lq2. (*E*) K_i values (mean ± SEM; $n = 6-10$) for the wild-type and mutant Lq2 are summarized. K_i values were estimated using the leak-subtracted data, as described in the Figure 5 legend. Panel F summarizes the free energy changes (in RT units) due to the Lq2 mutations. (G) An NMR structural model for charybdotoxin (*27*). The residues corresponding to the four Lq2 residues, mutated in this study, were highlighted using van der Waals surfaces. (H) Amino acid sequence of CTX and LQ2 in single letter code.

predictions from work on the voltage- and Ca^{2+}-activated K^+ channels: Two of the three interaction surface residues had a large effect when mutated, and Arg 19 (on the predicted back-side) was silent.

DISCUSSION

Previous studies on pore-blocking scorpion toxins have provided a detailed description of the way in which these inhibitors interact with voltage- and Ca^{2+}-activated K^+ channels. Scanning mutagenesis and thermodynamic mutant cycle structural analysis have allowed us to begin to envision what the interface of a toxin−channel complex looks like (*16*−*22*). In the present study, we sought to identify a protein ligand directed against an inward-rectifier channel, as none had been identified for this entire class of K^+ channels. Lq2, the inhibitor of ROMK1 identified here, turns out to be one of the voltage- and Ca^{2+}-activated K^+ channel blockers with which we are so familiar (*10*, *13*). Although the mutagenic analysis carried out in this study is limited in scope, it appears that Lq2 interacts with the ROMK1 channel with an orientation that is similar to the interaction of Lq2

(and its toxin family members) with voltage- and Ca^{2+}-activated K^+ channels.

Based on their amino acid sequences, the inward-rectifier K^+ channels are structurally quite distinct from the voltage- and Ca^{2+}-activated K^+ channels. The former have only two hydrophobic (presumably transmembrane) amino acid stretches, while the latter have six (*2*). However, both have a P-region (or pore-loop) which contains the eight amino acid K^+ channel signature sequence (*14*). As far as we know, all K^+ channels have this sequence, and its amino acids are presented to a central pore in quadruplicate, because K^+ channels are tetramers (*3*−*5*). Mutagenesis studies tell us that the pore-loop amino acids form the K^+ selectivity filter (*14*, *23*). Thus, it would appear that the different classes of K^+ channels are related structurally in the following manner: They have essentially the same K^+-selective ion conduction pore, but differ elsewhere in order to account for their ability to gate in response to changes in membrane voltage, cytoplasmic Ca^{2+} concentration, or other cytoplasmic ligands. Therefore, it is not surprising to see the promiscuity displayed here by Lq2. The recognition of K^+ channels from different classes by Lq2 is merely confirmation that their three dimensional K^+ pore structures are similar.

An interesting feature of the interaction between K^+ channels and scorpion toxins is that the affinity is coupled to the occupancy of K^+ ions inside the pore (*24*). The effect of K^+ on the affinity is mediated through the toxin residue Lys 27, which is conserved among members of the toxin family (*25*). When this residue (Lys 27) was mutated in three different toxin family members, very large effects on affinity (>1000-fold) were observed in all cases (*16*, *17*, *19*−*21*, *25*, *26*). Here we observe a modest effect of the K27A mutation. The significance of this finding is not clear at this point, but it implies that Lys 27 may not interact as intimately in the pore of an inward rectifier channel as it does in voltage- and Ca^{2+}-activated K^+ channels. Further studies are necessary to address this point.

In summary, we have purified a protein inhibitor of an inward-rectifier K^+ channel and found that it is Lq2, also an inhibitor of voltage- and Ca^{2+}-activated K^+ channels. This ligand should serve as a useful tool for studying ROMK1 channel function and for assessing the viability of ROMK1 channels expressed and purified for structural studies.

ACKNOWLEDGMENT

We thank K. Ho and S. Hebert for the ROMK1 cDNA, L. Jan for the IRK1 cDNA, M. Garcia for recombinant CTX, IbTx, and MgTx, J. Lewis for assistance in preparing recombinant Lq2, and J. Rush (Harvard HHMI Biopolymer Facility) for performing amino acid analysis and mass spectrometry. We also thank C.-S. Park, P. Hidalgo, C. Miller, and K. Swartz for helpful discussions.

REFERENCES

1. Adams, M. E., and Swanson, G. (1994) *TINS Suppl.*, 1−29.
2. Jan, L. Y., and Jan, Y. N. (1994) *Nature 371*, 119−122.
3. MacKinnon, R. (1991) *Nature 350*, 232−235.
4. Liman, E. R., Tytgat, J., and Hess, P. (1992) *Neuron 9*, 861−871.
5. Yang, J., Jan, Y. N., and Jan, L. Y. (1995) *Neuron 15*, 1441−1447.
6. Ho, K., Nichols, C. G., Lederer, W. J., Lytton, J., Vassilev, P. M., Kanazirska, M. V., and Hebert, S. C. (1993) *Nature 362*, 31−38.
7. Kubo, Y., Baldwin, T. J., Jan, Y. N., and Jan, L. Y. (1993) *Nature 362*, 127−132.
8. Garcia, M. L., Garcia-Calvo, M., Hidalgo, P., Lee, A., and MacKinnon, R. (1994) *Biochemistry 33*, 6834−6839.
9. Park, C.-S., Hausdorff, S. F., and Miller, C. (1991) *Proc. Natl. Acad. Sci. U.S.A. 88*, 2046−2050.
10. Escobar, L., Root, M. J., and MacKinnon, R. (1993) *Biochemistry 32*, 6982−6987.
11. Lu, Z., and MacKinnon, R. (1994) *Nature 371*, 243−246.
12. Wible, B. A., Taglialatela, M., Ficker, E., and Brown, A. M. (1994) *Nature 371*, 246−249.
13. Lucchesi, K., Ravindran, A., Young, H., and Moczydlowski, E. (1989) *J. Membrane Biol. 109*, 69−281.
14. Heginbotham, L., Lu, Z., Abramson, T., and MacKinnon, R. (1994) *Biophys. J. 66*, 1061−1067.
15. Schwalbe, R. A., Wang, Z., Wible, B. A., and Brown, A. M. (1995)*J. Biol. Chem. 270*, 15336−15340.
16. Park, C.-S., and Miller, C. (1992) *Biochemistry 31*, 7749−7755.
17. Stampe, P., Kolmakova-Partensky, L., and Miller, C. (1994) *Biochemistry 33*, 443−450.
18. Goldstein, S. A. N., Pheasant, D. J., and Miller, C. (1994) *Neuron 12*,1377−1388.
19. Hidalgo, P., and MacKinnon, R. (1995) *Science 268*, 307−310.
20. Ranganathan, R., Lewis, J. H., and MacKinnon, R. (1996) *Neuron 16*, 131−139.
21. Aiyar, J., Withka, J. M., Rizzi, J. P., Singleton, D. H., Andrews, G. C., Lin, W., Boyd, J., Hanson, D. C., Simon, M., Dethlefs, B., Lee, C. L., Hall, J. E., Gutman, G. A., and Chandy, K. G. (1995) *Neuron 15*, 1169−1181.
22. Naranjo, D., and Miller, C. (1996) *Neuron 16*, 123−130.
23. Heginbotham, L., Abramson, T., and MacKinnon, R. (1992) *Science 258*, 942−944.
24. MacKinnon, R., and Miller, C. (1988) *J. Gen. Physiol. 91*, 335−349.
25. Park, C.-S., and Miller, C. (1992b) *Neuron 9*, 307−313.
26. Goldstein, S. A. N., and Miller, C. (1993) *Biophys. J. 65*, 1613−1619.
27. Bontems, F., Gilquin, B., Roumestand, C., Menez, A., and Toma, F. (1992) *Biochemistry 31*, 7756−7764.

BI9702849